中国激光

单个阿秒脉冲表征技术研究进展

王家灿[1,2]，肖凡[1,2]，王小伟[1,2**]，王力[1,2]，陶文凯[1,2]，赵零一[1,2]，李悉奥[1,2]，赵增秀[1,2*]

[1]国防科技大学理学院，湖南 长沙 410073；

[2]极端条件物理及应用湖南省重点实验室，湖南 长沙 410073

摘要 自本世纪初超快科学进入阿秒领域以来，阿秒脉冲以其超宽频谱和超短时间分辨，为研究阿秒时间尺度的瞬态过程提供了有力工具，推动了人们对光与物质相互作用以及微观超快动力学机制的理解。基于高次谐波的单个阿秒脉冲产生技术已日臻成熟，通过发展多种时空选通门技术，阿秒脉冲脉宽不断缩短，已达到的最短纪录为43 as。相较于阿秒脉冲的产生，对其精确测量与表征是深入研究和应用的基础，目前主流表征方法是通过阿秒条纹相机技术测量获得条纹能谱，进而从中提取阿秒脉冲的时域信息。首先简要回顾了高次谐波产生、单个阿秒脉冲选通及测量的发展，然后介绍了阿秒条纹相机技术的原理，并重点阐述了基于阿秒条纹能谱的表征算法，对其主要优缺点进行分析，最后对阿秒脉冲表征的发展进行了总结和展望。

关键词 非线性光学；单个阿秒脉冲；阿秒条纹相机；相位反演与表征

中图分类号 O437 **文献标志码** A **DOI**：10.3788/CJL231535

1 引 言

观测和研究瞬态过程是人们探索未知和认识自然的重要手段。超短超强脉冲的出现，为人们以极高时间分辨研究微观超快动力学过程提供了可能，推动了人们对光与物质相互作用机理的理解。微观范畴内，分子转动过程时间尺度在皮秒量级，分子振动过程时间尺度在飞秒量级。Zewail[1]将飞秒激光应用于超快成像技术，分析出分子中原子在化学反应中的运动轨迹，使人们能够理解和研究重要化学反应过程，从而开创了飞秒化学。而原子、分子、固体中电子运动时间尺度为阿秒量级，需要阿秒宽度的超短脉冲对其进行测量和研究。

在强激光场作用于气体原子的实验中，人们观测到基频光的高次谐波辐射（HHG）[2-3]。Corkum[4]于1993年提出了半经典三步模型，从理论上解释了惰性气体原子HHG的产生原理，为理解HHG现象提供了既简洁又清晰的物理图像。之后人们深入研究了气相离子、液体、固体的HHG机理及应用[5-13]。本质上高次谐波是一系列时间上周期排列的阿秒脉冲串，为了获得单个阿秒脉冲（IAP），可以在驱动激光作用的大部分时间里破坏辐射高次谐波的必要条件，只在半个周期里允许HHG发射，这个发射的时间窗口即称为选通门[14-19]。结合HHG和适当的选通门技术，人们已经可以产生脉宽为数百阿秒甚至几十阿秒的激光脉冲。

2001年，Agostini小组Paul等[20]使用40 fs钛宝石激光器作用于氩气，产生并表征了脉冲宽度为250 as的13～19阶高次谐波的阿秒脉冲串。同年，Krausz小组Hentschel等[21]使用7 fs少周期红外（IR）脉冲得到了脉宽为650 as的单个阿秒脉冲，标志着超快研究进入阿秒领域。其后20多年来，阿秒脉冲脉宽被不断压缩，国内外的单个阿秒脉冲产生研究均取得重要进展（见图1）[22-32]。2023年，美国科学家Pierre Agostini、德国科学家Ferenc Krausz和瑞典科学家Anne L'Huillier被授予诺贝尔物理学奖，以表彰他们在实验上产生阿秒脉冲串及单个阿秒脉冲，以及将阿秒脉冲用于研究物质中电子动力学过程的巨大贡献。

阿秒脉冲的脉冲宽度已达到几十阿秒的时间尺度，光谱范围覆盖了紫外、极紫外（XUV）至软X射线（SXR）波段[33-36]。基于阿秒瞬态吸收光谱、阿秒光电子测量等技术，阿秒脉冲被广泛应用于对原子、分子和凝聚态物质中的电子超快动力学过程进行研究，如俄歇衰变[37]、原子内壳层跃迁[38]、原子分子光电离延时[39-42]、多原子分子内的电子转移[43-47]、固体材料中的超快结构相变[48]、宽禁带半导体中光诱导的拍赫兹振荡调控[49-51]以及液体环境中的超快质子转移过程等[52-53]。

收稿日期：2023-12-16；**修回日期**：2024-01-20；**录用日期**：2024-02-01；**网络首发日期**：2024-02-20

基金项目：国家重点研发计划（2019YFA0307703）、国家自然科学基金（12234020，11974426）、国家自然科学基金重大研究计划（91850201）

通信作者：*zhaozengxiu@nudt.edu.cn；**xiaowei.wang@nudt.edu.cn

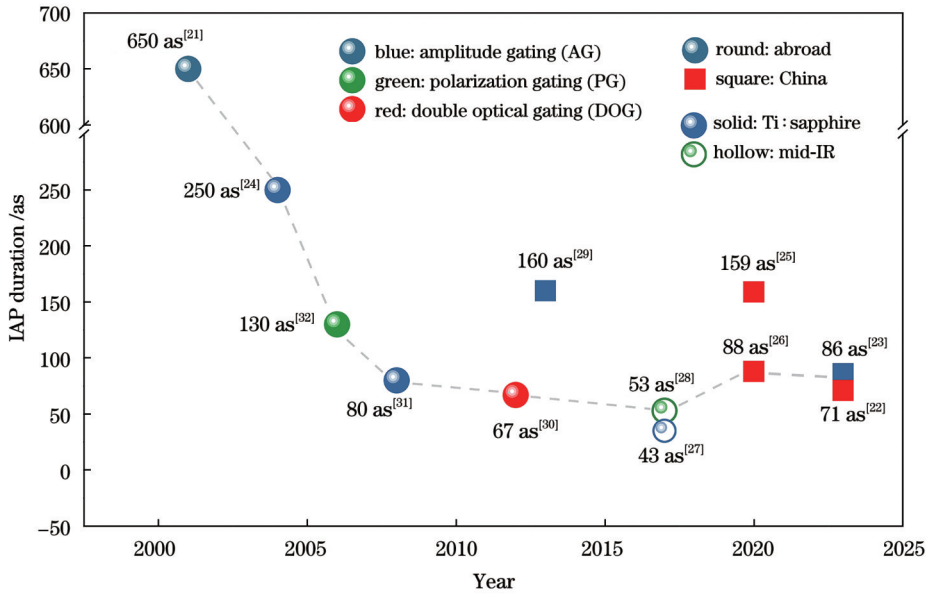

图 1　单个阿秒脉冲产生技术的发展历史

Fig. 1　Development of generation techniques for isolated attosecond pulse

对单个阿秒脉冲的光谱、相位、脉宽、波形等特性进行准确表征是重要且富有挑战性的课题。时间尺度上，阿秒脉冲脉宽远小于电子元件纳秒量级的最快响应时间，脉宽为几十阿秒甚至更短的阿秒脉冲已经达到极紫外或软X射线波段。由于极紫外波段光脉冲的光子在非线性介质中会发生强烈吸收，缺少合适的非线性介质进行响应与测量，传统的飞秒脉冲测量技术无法直接推广到阿秒领域，因此准确表征阿秒脉冲一直很具挑战性。由于目前阿秒脉冲能量较低，主流方法是将阿秒脉冲与飞秒脉冲进行互相关测量，即利用阿秒脉冲与飞秒脉冲共同作用于气体介质，通过电离的电子在飞秒激光场中的运动特性反演阿秒脉冲信息。

2001年，Paul等[20]开创性地提出使用基于双光子跃迁干涉的阿秒脉冲串重构技术（RABBITT），利用红外激光调制阿秒脉冲电离气体产生的光电子，当红外光足够强时会出现边带峰，随着两束激光相对延时的变化，边带能谱强度出现周期性调制，从这种能谱的调制中可以获得各频率成分的相对相位，进而实现对阿秒脉冲串的表征和重建。

为了获得百阿秒甚至更短的时间分辨，实验上需要从阿秒脉冲串中选通出单个阿秒脉冲。单个阿秒脉冲的精确表征比阿秒脉冲串更加复杂。由于阿秒脉冲的光谱可以从实验中直接测量，因此阿秒脉冲的时域表征本质上是阿秒脉冲的光谱相位测量问题。根据测量位置的不同，单个阿秒脉冲的测量方法可以分为原位测量和离位测量。原位测量包括：1）依赖于三步模型中回碰电子辐射光子所携带的阿秒脉冲信息进行反演[54]；2）空间分离的阿秒灯塔[55-57]和华中科技大学陆培祥课题组于2020年提出的全光阿秒测量方法[58-60]。离位测量主要包括：1）基于高次谐波光谱干涉的超短脉冲电场的重建算法（SPIDER）[61-62]；2）基于阿秒脉冲和红外脉冲互相关光电子探测的阿秒条纹相机技术[63]。

阿秒条纹相机技术是目前单个阿秒脉冲测量的主流手段。在传统条纹相机的基础上，Itatani等[63]于2002年提出将横向偏转电场换成随时间变化更快的飞秒激光电场。电子被阿秒脉冲电离后在飞秒脉冲作用下受到调制，这种能谱调制随阿秒-飞秒光场的延迟而变化，阿秒脉冲相位信息就编码在其中，通过合适的算法能够从中反演出阿秒脉冲的频谱相位，进而重建阿秒脉冲时域电场，此即阿秒条纹相机技术。

受益于单个阿秒脉冲前所未有的时间分辨能力，单个阿秒脉冲的测量技术在近年来得到快速发展[64-74]。本文主要简述从阿秒条纹相机条纹能谱中表征阿秒脉冲时域特性的研究进展。首先简述阿秒条纹相机技术原理，然后介绍单个阿秒脉冲表征算法的研究进展，最后对单个阿秒脉冲的表征技术进行总结和展望。

2　阿秒条纹相机技术

条纹相机技术最初被用于测量皮秒量级的超快光信号，主要思想是利用随时间变化的横向电场偏转光电子轨迹，将脉冲信号的时间信息转换到探测器的空间分布上，通过测量光电子的空间分布能够反演待测脉冲随时间的强度分布。为了测量时间尺度更短的阿秒脉冲，Itatani等[63]提出将横向偏转电场换成随时间变化更快的飞秒激光场。如图2所示，在阿秒条纹相机中，阿秒脉冲电离气体原子产生的光电子在红外光场中加速，其光电子能量改变量由电离时刻的激光场

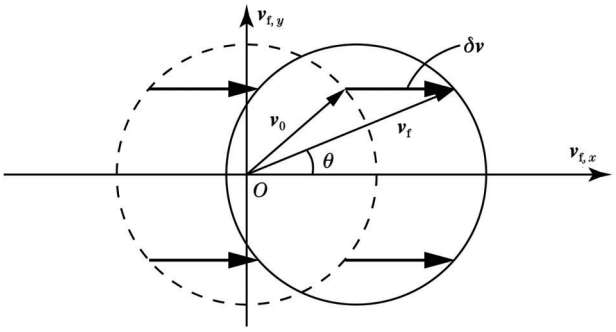

图 2　阿秒脉冲电离的光电子在强激光场作用下的速度改变。虚线表示无强激光场时的速度分布，实线表示强激光场作用时的速度分布[63]

Fig. 2　Effect of strong laser field on photoelectrons ionized by attosecond pulses. Dashed line presents velocity distribution without laser field while solid line with laser field[63]

相位决定，等效于在时域上引入相位调制。采用合适的反演算法，可以从条纹能谱中测量阿秒脉冲的光谱相位，进而结合光谱振幅重建时域电场，实现对阿秒脉冲的时域表征。

当探测方向与驱动光偏振方向平行时，电子被阿秒脉冲电离到连续态后，在驱动光场作用下的速度和最终的动能改变量可以表示为

$$\boldsymbol{v}(t)=-\int\frac{e}{m_e}\boldsymbol{E}_L(t)\mathrm{d}t+\left[\boldsymbol{v}_0+\frac{e}{m_e}\boldsymbol{A}_L(t_i)\right]=-\frac{e}{m_e}\boldsymbol{A}_L(t)+\left[\boldsymbol{v}_0+\frac{e}{m_e}\boldsymbol{A}_L(t_i)\right],\tag{1}$$

$$\Delta K(\tau)\approx\sqrt{8U_P(\tau)K_i}\sin\left(\omega_L\tau+\varphi\right)=-A_L(\tau)\sqrt{\frac{2e^2}{m_e}K_i},\tag{2}$$

式中：$\boldsymbol{E}_L(t)$和$\boldsymbol{A}_L(t)$分别为红外光脉冲的电场和矢势；$\boldsymbol{v}_0$为电子电离后的初速度；e和m_e分别表示电子电荷和质量；t_i为电子的电离时刻；$-(e/m_e)\boldsymbol{A}_L$表示电子在电场中振荡运动且在激光场结束时变为零，最终电子动量取决于电离时刻的电场矢势和初始动量；$U_P=e^2E_0^2(\tau)/4m_e\omega_L^2$表示红外激光场有质动力能；$K_i$为光电子初始动能；$\omega_L$为驱动光频率；$\varphi$表示红外光场与阿秒脉冲的相对相位。

光电子条纹能谱是关于电子动能及扫描延时的二维函数。当红外激光场为圆偏振时，将产生角度分辨的光电子谱，也可用于重建阿秒脉冲，以及进行自由电子激光的单发测量[75-78]。

图 3(a)是一种实验上常见的基于阿秒条纹相机技术的光路示意图，被广泛应用于各种阿秒光学实验[21-22,26,28,31-32,79-80]。实验中，入射红外脉冲被分为两束，其中泵浦光在气体池中产生的阿秒脉冲被轮胎镜聚焦后，透过百纳米厚度的金属薄膜，滤除红外驱动光并进行色散补偿后[81-86]，与探测光通过带孔合束镜合束，然后在气体喷嘴处产生受探测光调制的光电子。如图 3(c)所示，阿秒脉冲产生的光电子被飞秒脉冲调制后由飞行时间谱仪(TOF)收集并探测。扫描阿秒脉冲和飞秒脉冲的时间延迟，最终能够获得图 3(b)所示的条纹能谱图。通过合适的反演算法能够从中重建出阿秒脉冲和飞秒脉冲的时域信息，以及探测介质的光电离截面和光电离延时等信息[37,87]，也可用于研究

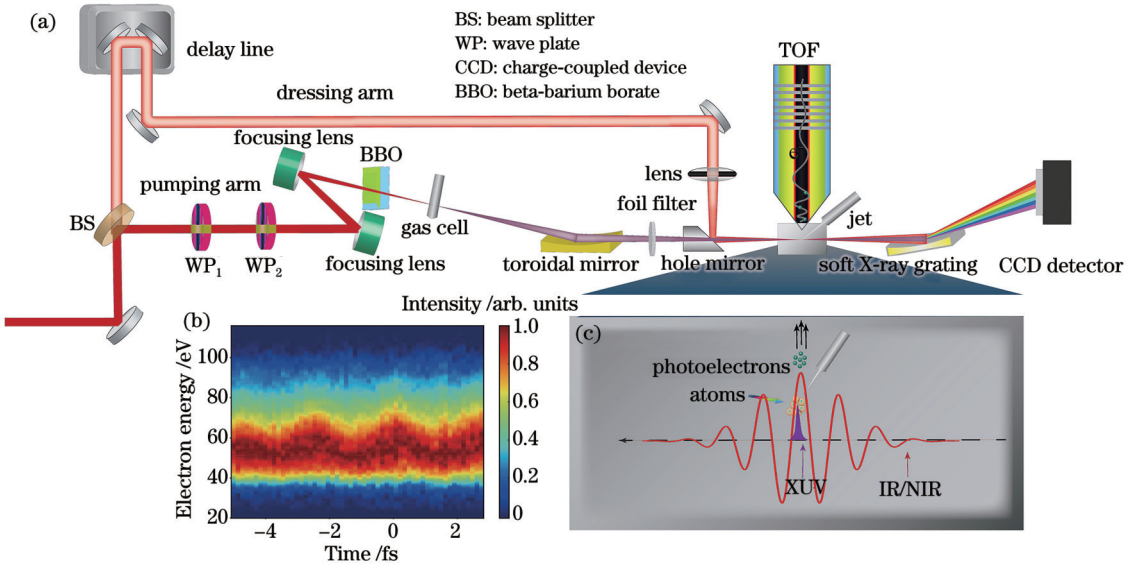

图 3　阿秒条纹相机技术。(a)阿秒条纹相机技术光路图；(b)实验测量的阿秒条纹能谱图；(c)电子被 XUV 脉冲从靶原子电离，在近红外(NIR)或红外电场中加速后，由 TOF 收集并探测

Fig. 3　Attosecond streaking camera scheme. (a) Attosecond streaking camera scheme diagram; (b) experimental streaking spectrogram of IAP; (c) ionized from noble gas atoms by XUV pulses, photoelectrons are then accelerated in infrared/near-infrared (IR/NIR) field and collected by TOF

气体[88-90]、固体中的阿秒时间尺度动力学过程[80]。

3 基于阿秒条纹谱图的相位重建

自阿秒条纹相机技术提出以来，已有许多反演方法能够从阿秒条纹谱图反演阿秒脉冲的光谱相位，进而重建阿秒脉冲时域波形，如用于阿秒脉冲重建的频率分辨光学门技术（FROG-CRAB）[91-92]、基于单频滤波的宽带阿秒脉冲表征算法（PROOF）[93]、基于层析成像原理的层析算法（ePIE）[94-96]、基于 Volkov 态的广义投影算法（VTGPA）[97]、将阿秒和红外脉冲以参数化形式描述从而直接通过迭代优化参数的反演算法（PROBP）[98-99]，以及将神经网络、机器学习应用于阿秒脉冲表征的算法等[100-102]。下面分别加以介绍。

3.1 FROG-CRAB

Mairesse 等[61,92]在 2005 年将成熟地应用于飞秒脉冲表征的频率分辨光学门（FROG）算法[103-104]引入阿秒领域，提出了用于阿秒脉冲重建的频率分辨光学门技术 FROG-CRAB。在飞秒脉冲测量中，FROG 谱图是光电子能量和时间延迟的二维函数，通常可以写为

$$S_{\mathrm{FROG}}(v,\tau)=\left|\int_{-\infty}^{\infty}G(t)E(t-\tau)\mathrm{e}^{\mathrm{i}\omega t}\mathrm{d}t\right|^2,\tag{3}$$

式中：$G(t)$为门脉冲；$E(t-\tau)$是与门脉冲具有时间延迟的待测脉冲。

原则上，一幅给定的谱图 S_{FROG} 与唯一待测脉冲和门脉冲对应，通过主成分广义投影算法（PCGPA）[105]进行迭代求解，可以重建门脉冲和待测脉冲的时域信息。其主要思想是首先根据实验参数和经验，设定一组 $P(t)$和 $G(t)$猜测值作为初始值，通过仿真模拟计算得到 S'_{FROG}，构造最小误差函数：

$$\varepsilon_{\mathrm{FROG}}=\left[\frac{1}{N^2}\sum_{i=1}^{N}\sum_{j=1}^{N}\left[S'_{\mathrm{FROG}}(v,\tau)-S_{\mathrm{FROG}}(v,\tau)\right]^2\right]^{1/2}。\tag{4}$$

在每步迭代计算中，保留使得误差函数更小的优化 $P(t)$和 $G(t)$，直至误差精度收敛到设定目标时，将最后一步迭代的 $P(t)$和 $G(t)$作为求解结果。

在阿秒脉冲测量的 FROG-CRAB 中，引入红外飞秒脉冲作为门脉冲，根据强场近似理论（SFA），忽略中间激发态的相互作用，假设电子从基态直接电离到连续态，并假设电子电离后只受到激光场作用，即忽略离子势对电子的影响，当探测方向与阿秒脉冲及红外脉冲偏振方向相同时，二维光电子条纹谱图可以写作

$$S(v,\tau)=\left|\int_{-\infty}^{\infty}E_{\mathrm{X}}(t)d_{\mathrm{p}}(t)\mathrm{e}^{\mathrm{i}\phi(v,t-\tau)}\mathrm{e}^{-\mathrm{i}(W+I_{\mathrm{P}})t}\mathrm{d}t\right|^2,\tag{5}$$

$$\phi(v,t)=-\int_{t}^{\infty}\left[vA_{\mathrm{L}}(t')+A_{\mathrm{L}}^2(t')/2\right]\mathrm{d}t',\tag{6}$$

式中：$E_{\mathrm{X}}(t)$为阿秒脉冲电场；$d_{\mathrm{p}}(t)$为气体介质电离的跃迁矩阵元；W为光电子动能；I_{P}为测量气体原子的电离能；$\phi(v,t)$为飞秒脉冲对光电子引入的相位调制。

为了将飞秒脉冲测量 FROG 算法引入阿秒脉冲测量，通过对比式（3）和式（5）可以将 $E_{\mathrm{X}}(t)$视为待测脉冲，$\phi(v,t)$为参考门脉冲，它是动量 v 和延迟时间 t 的二元函数。引入假设 $\phi(v,t)=\phi(v_0,t)$，其中 v_0 为光电子中心能量，这种假设称为中心动量近似（CMA）。

采用 FROG-CRAB 这样的迭代算法，可以从实验谱图中反演得到飞秒脉冲和阿秒脉冲的光谱相位，继而重建时域波形。2006 年 Sansone 等[32]在实验上测量了阿秒条纹谱图，并首次使用 FROG-CRAB 算法表征获得了脉宽 130 as 的单个阿秒脉冲，之后该算法继续拓展优化[60,91]并广泛应用于阿秒脉冲表征[23,26,29-32]。2022 年 Takahashi 课题组首次报道产生了 0.24 μJ 桌面式阿秒脉冲源，采用 FROG-CRAB 算法表征获得了 266 as 的单个阿秒脉冲，实现了桌面式 10 Hz 低重复频率、1.1 GW 高强度的单个阿秒脉冲源[106]。但随着驱动光强的提高、选通门技术的进步和驱动光波长的提高，阿秒脉冲光谱逐渐变宽且向软 X 射线波段发展。对于脉冲更短、光谱更宽的阿秒脉冲，CMA 逐渐失效，导致 FROG-CRAB 算法的误差变大。

3.2 层析算法

在 FROG-CRAB 算法的基础上，为了克服其傅里叶变换带来的精度和谱宽限制，并提高反演算法的迭代速度，Lucchini 等[94-96]结合 CMA，首次将 ePIE 应用于表征阿秒脉冲，并扩展到反演紫外至极紫外的宽带阿秒脉冲振幅和光谱相位，该算法被称为 rePIE。

ePIE 是一种最早由 Hoppe[107]提出用于岩层造影的相位反演方法，并于 2007 年首次在实验上实现无透镜方案的可见光波段相位提取[108]。该方法基于远场散射的测量结果（如光谱或电子谱），通过对待测波形传播路径上的每个横向切面进行迭代求解，重建实空间中波形的振幅和相位。Lucchini 等[94-96]将 ePIE 算法与阿秒条纹相机技术相结合，通过迭代求解（ePIE、rePIE），从条纹谱图 $S(\omega,\tau)$中同时实现对阿秒脉冲和飞秒脉冲的表征。该算法将阿秒条纹相机技术中的红外脉冲场视为门脉冲，可用类似式（6）的形式表示：

$$P(t)=\exp\left\{-\mathrm{i}\int_{t}^{\infty}\mathrm{d}t'\left[p_{\mathrm{c}}A_{\mathrm{L}}(t')-\frac{A_{\mathrm{L}}^2(t')}{2}\right]\right\},\tag{7}$$

式中：$P(t)$为红外脉冲场引起的调制项；p_{c}表示未被调制的中心动量。

层析算法中首先给出阿秒脉冲和红外脉冲的猜测初始值，然后进行寻优迭代，第 j 次迭代根据延迟 τ_n 下 XUV 脉冲 $E_{j,n}(t)$和门脉冲 $P_{j,n}(t)$，可以定义复合场

$$\xi_{j,n}(t,\tau_n)=E_{j,n}(t)P_{j,n}(t-\tau_n)。\tag{8}$$

将 $\xi_{j,n}(t,\tau_n)$进行傅里叶变换得到频域分布 $\xi_{j,n}(\omega,\tau_n)$，使用谱图 $S(\omega,\tau)$替换其振幅并保留相位，再通过傅里叶逆变换得到新的复合场 $\xi'_{j,n}(t,\tau_n)$。然后迭代优化得到第 $j+1$ 次阿秒脉冲 $E_{j+1,n}(t)$和门脉冲 $P_{j+1,n}(t)$。如此多次迭代直至收敛，进而同时实现阿

秒脉冲和红外脉冲时域波形的重建。

不同于PCGPA或最小二乘广义投影算法(LSGPA)等投影算法,层析投影算法放宽了对条纹相机测量能谱数据的频率分辨率和时间延迟精度的要求,大大减小了实验测量和迭代计算中的数据规模,提高了反演速度和精度。ePIE与PCGPA和LSGPA的对比如图4所示。但其仍采用了中心动量近似,不适用于宽带阿秒脉冲的测量。

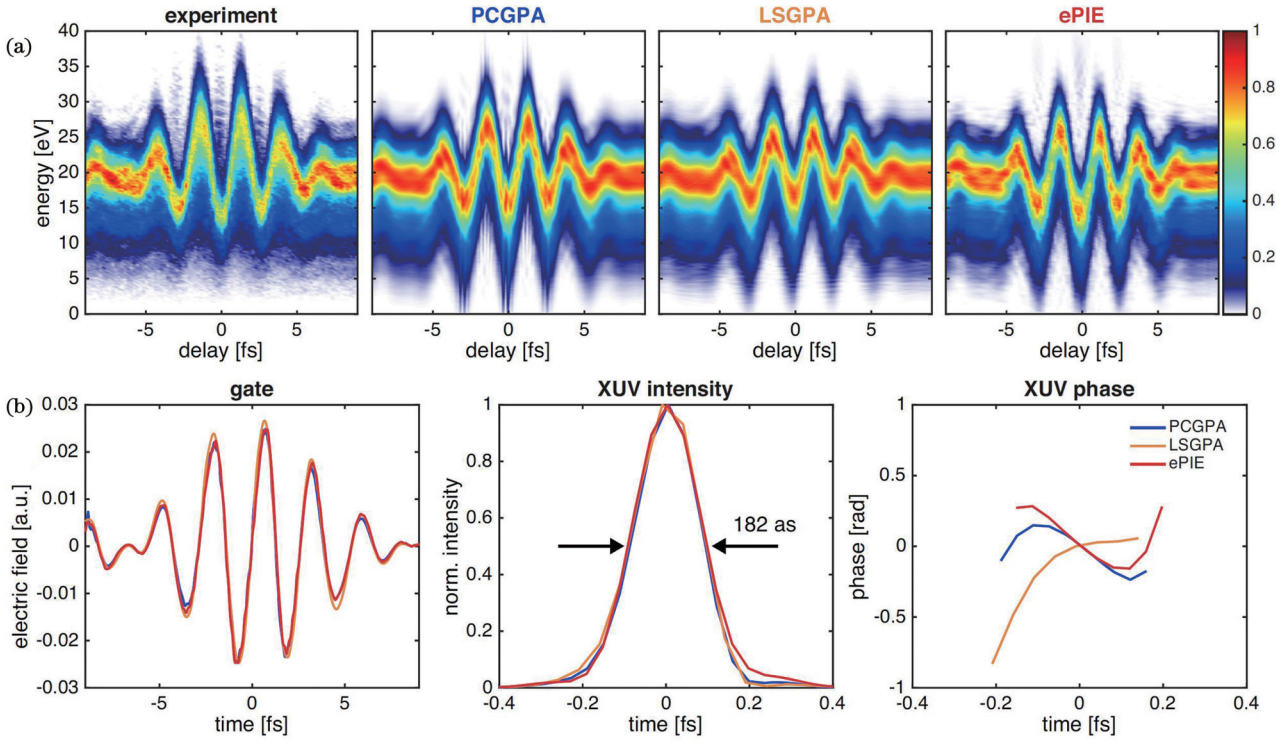

图4　PCGPA、LSGPA和ePIE反演实验条纹谱图结果对比。(a)三种算法20000次迭代反演阿秒条纹谱图与实验阿秒条纹谱图对比;(b)三种算法反演得到的红外电场、阿秒脉冲包络和相位[96]

Fig. 4　Characterization of PCGPA, LSGPA and ePIE for experimental spectrogram. (a) Reconstruction results with 20000 iterations from PCGPA, LSGPA and ePIE, together with experimental result; (b) retrieved NIR streaking fields, XUV pulse envelope intensities and phases from PCGPA, LSGPA and ePIE[96]

3.3　PROOF

为了克服中心动量近似的局限性,Chini等[93]于2010年提出基于单频滤波的宽带阿秒脉冲表征算法PROOF,其原理如图5所示。该算法能够在弱调制场($<10^{12}$ W/cm^2)条件下反演宽带光谱单个阿秒脉冲。当红外调制场较弱时,可以采用类似RABBITT中的低阶微扰方法处理,只考虑调制脉冲对阿秒光电子的单光子调制,并忽略高阶过程,式(5)所描述的光电子谱图简化为3项:

$$I(v,\tau)=I_0(v)+I_{\omega_L}(v,\tau)+I_{2\omega_L}(v,\tau),\tag{9}$$

式中:ω_L为驱动场频率;τ为阿秒脉冲和飞秒脉冲的时间延迟;$I_0(v)$为零频项,不随时间延迟振荡;$I_{\omega_L}(v,\tau)$和$I_{2\omega_L}(v,\tau)$与光子跃迁通道干涉有关,分别随延迟以基频ω_L和倍频$2\omega_L$振荡。

假设驱动光为线偏振场,且满足慢变包络近似,也即$\varepsilon_L(t)=E_0(t)\cos(\omega_L t)$。当光场较弱时($vE_0/2\omega_L\ll\omega_L$),基频项为

$$I_{\omega_L}(v,\tau)=U^2(\omega_v)\frac{vE_0}{\omega_L}\gamma(v)\sin[\omega_L\tau+\alpha(v)],\tag{10}$$

$$\gamma(v)=\frac{I(\omega_v+\omega_L)+I(\omega_v-\omega_L)}{I(\omega_v)}-2\frac{\sqrt{I(\omega_v+\omega_L)I(\omega_v-\omega_L)}}{I(\omega_v)}\cos\left[\phi(\omega_v-\omega_L)+\phi(\omega_v+\omega_L)\right],\tag{11}$$

$$\tan\left[\alpha(v)\right]=\frac{\sqrt{I(\omega_v+\omega_L)}\sin\left[\phi(\omega_v)-\phi(\omega_v+\omega_L)\right]-\sqrt{I(\omega_v-\omega_L)}\sin\left[\phi(\omega_v-\omega_L)-\phi(\omega_v)\right]}{\sqrt{I(\omega_v+\omega_L)}\cos\left[\phi(\omega_v)-\phi(\omega_v+\omega_L)\right]-\sqrt{I(\omega_v-\omega_L)}\cos\left[\phi(\omega_v-\omega_L)-\phi(\omega_v)\right]},\tag{12}$$

式中:ω_v为阿秒脉冲光子频率。

从式(10)可以看出,基频项为正弦振荡,具有调制深度$\gamma(v)vE_0/\omega_L$和相位角$\alpha(v)$,二者均含有阿秒脉冲的相位信息。但实验中调制深度通常具有测量噪声,不利于精确的阿秒脉冲重建。相比之下,相位角可以通过多周期调制的平均以减小噪声的影响。通过构造相位角$\alpha(v)$的最小误差函数,采用遗传算法求解式(12),可以重建阿秒脉冲的时域波形。

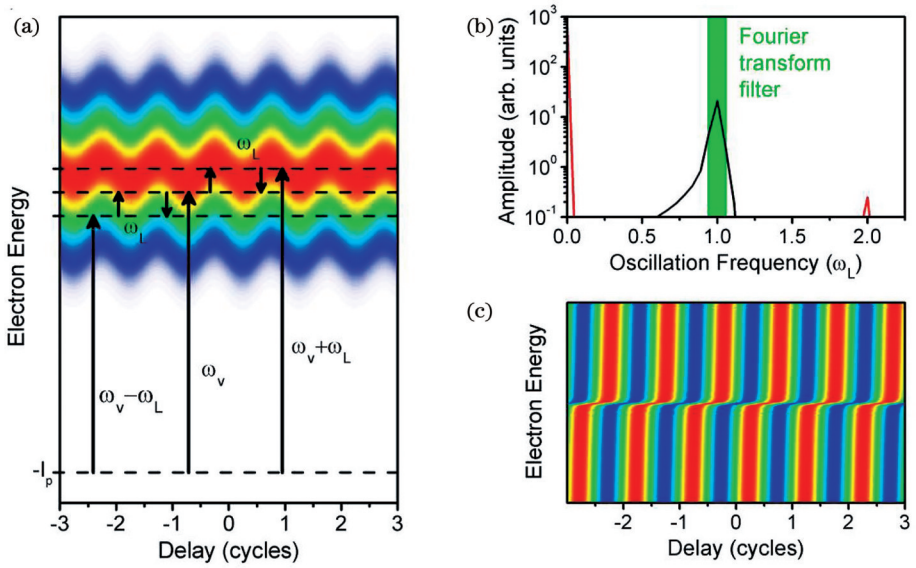

图 5　PROOF 原理图。(a)单个阿秒脉冲电离基态电子至连续态，红外脉冲调制连续态的电子形成随时间延迟的振荡；(b)对特定能量的光电子信号进行傅里叶变换的频率信号，在激光频率的零频、基频和倍频处存在信号峰，对基频信号进行选通；(c)基频信号进行傅里叶逆变换的谱图，包含相位角信息[93]

Fig. 5　Diagram of PROOF. (a) Photoelectrons are ionized from ground states to continuum by IAP. Continuum states separated by laser frequency are coupled, leading to oscillation of spectrogram with time delay. (b) Signal peaks by Fourier transform from photoelectrons in (a) at certain energy, lying at laser frequencies of zero, ω_L and $2\omega_L$, whereas ω_L oscillation component is selected by using band-pass filter. (c) Spectrogram retrieved from inverse Fourier transform of filtered ω_L component of oscillation, which encodes phase angle $\alpha(v)$[93]

相较 FROG-CRAB，PROOF 方法更为简洁。该方法只考虑单光子调制项，降低了反演复杂度，更适合宽带光谱、弱光强调制的阿秒脉冲反演，自提出以来得到了持续发展[22,109]和广泛应用[25,28,30]。如图 6 所示，常

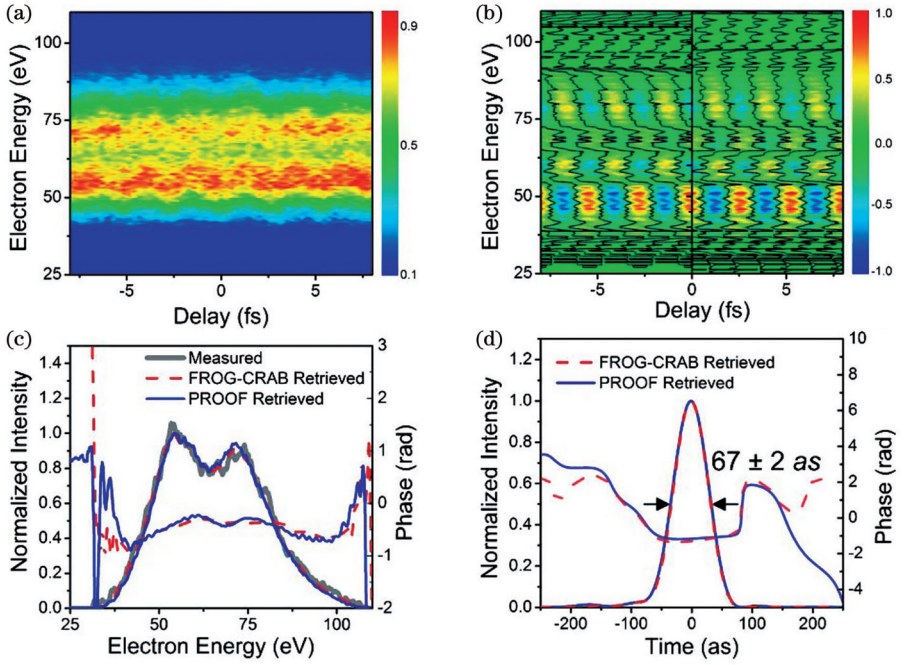

图 6　67 as 单个阿秒脉冲测量与表征。(a)实验测量阿秒光电子条纹谱图；(b)实验谱图(a)中提取的基频信号(左)与反演所得基频信号(右)对比；(c)实验测量光电子谱(粗实线)，PROOF 反演谱和相位(实线)，以及 FROG-CRAB 反演谱和相位(虚线)；(d)PROOF(实线)和 FROG-CRAB(虚线)重建的阿秒时域波形与相位[30]

Fig. 6　Characterization of 67 as IAP. (a) Experimentally obtained streaking electron spectrogram; (b) comparison of filtered I_{ω_L} component (left) with retrieved one (right); (c) experimental photoelectron spectrum (thick solid), PROOF retrieved spectra and phase (solid) and FROG-CRAB ones (dashed); (d) reconstructed temporal profiles and phases by PROOF (solid) and FROG-CRAB (dashed)[30]

增虎课题组于2012年报道了使用7 fs近红外脉冲结合双光学门技术，获得55～130 eV超连续光谱，采用PROOF表征脉宽为67±2 as的单个阿秒脉冲，与FROG-CRAB反演结果互相印证[30]。

然而，PROOF采用的遗传算法在迭代求解时需要大量算力及时间，且算法对诸多实验条件的适应性讨论较少。在PROOF算法单频滤波的基础上，我们提出针对宽带阿秒脉冲的快速反演算法qPROOF[22]，有助于在超短阿秒脉冲产生实验中，为调整色散补偿和其他实验参数提供实时反馈。

在PROOF中，通过从条纹谱图中提取单频振荡成分（OOF）的相位角α，并利用其正切值来求解阿秒脉冲相位。这种做法会导致相位角α限制于$\left[-\pi/2,\pi/2\right]$，使得该算法无法准确反演有相位跳变的阿秒条纹谱。在一种改进的PROOF算法中[109]，同时使用单频调制信号的正切项$\tan\alpha$和振幅项A_i，通过迭代求解光谱相位差δ_i。然而在飞行时间谱仪探测光电子过程中，振幅项A_i通常噪声较大，在迭代过程中会逐渐积累反演误差，导致最终反演准确性难以保证。为了克服相位角求解过程中的误差并提高反演速度，qPROOF将相位角的正弦和余弦结合，定义新的误差函数，将相位角α拓展至$\left[-\pi,\pi\right]$区间，提高了对阿秒光谱相位跳变的检验能力。此外，这种处理可以解析地求出误差函数的微分形式，相比于遗传算法在寻找最优解过程中的随机性，qPROOF误差函数的微分形式为优化过程指明了方向。另外，采用拟牛顿算法BFGS，使得优化过程能够在数秒内快速收敛。qPROOF与PROOF的对比如图7所示。

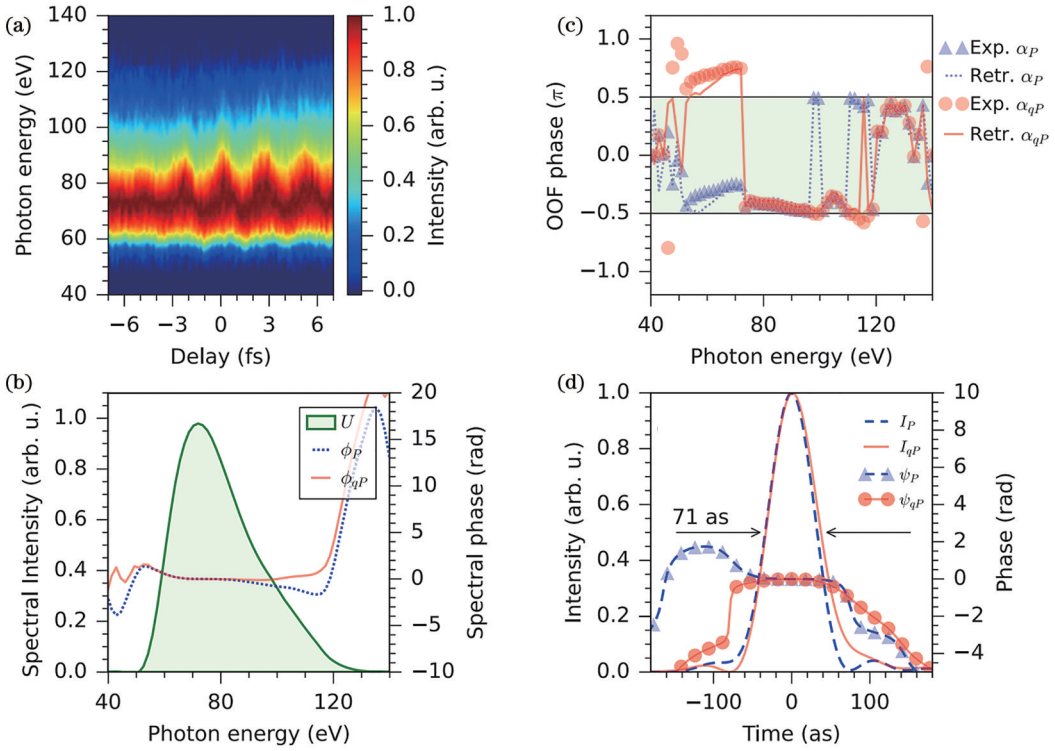

图7　PROOF和qPROOF表征71 as单个阿秒脉冲。(a)实验测量阿秒条纹谱图；(b)阿秒脉冲光谱以及PROOF和qPROOF重建频谱相位；(c)PROOF和qPROOF从条纹能谱中提取（Exp.）与反演（Retr.）OOF相位对比（α_P和α_{qP}分别对应PROOF和qPROOF）；(d)PROOF与qPROOF重建阿秒脉冲时域波形与时域相位[22]

Fig. 7　Reconstruction of 71 as experimental IAP by PROOF and qPROOF. (a) Experimental IAP spectrogram; (b) IAP spectrum and retrieved spectral phases by PROOF (solid line) and qPROOF (dashed line); (c) experimental extracted (Exp.) and retrieved (Retr.) OOF phases by PROOF (α_P) and qPROOF (α_{qP}); (d) reconstructed IAP temporal envelopes from PROOF (dashed line) and qPROOF (solid line), and retrieved temporal phases from PROOF (blue triangles) and qPROOF (red circles)[22]

详细的数值实验验证了qPROOF算法对于宽带阿秒脉冲反演的有效性以及优于PROOF的相位跳变处理能力。在给定宽带阿秒脉冲光谱及相位的情况下，测试红外脉冲脉宽及光强的反演结果也表明qPROOF拓宽了红外脉冲脉宽及光强范围，能够适用于3 fs以上，光强在10^{13} W/cm^{2}以下的少周期红外调制场。同时对于实验设备本身的固有噪声，如飞行时间谱仪的测量噪声、主动相位锁定时间抖动及扫描步长等因素也具有良好的鲁棒性。

3.4　VTGPA

绕开CMA的另一种思路是在式(5)的计算中不采用傅里叶变换，而是直接数值求解积分。Keathley等[97]提出了基于Volkov态的广义投影算法VTGPA，该算法根据式(5)中的跃迁振幅表达式直接计算条纹谱图，并采用最小误差函数进行寻优求解，绕过傅里叶变换的同时，也避免了FFT对能谱数据中时间和能量

采样精度的限制以及数据插值的复杂过程。

VTGPA 算法中，第一步给出一组试探阿秒脉冲和红外调制场矢势作为迭代初值，然后代入基于 SFA 的跃迁振幅表达式，计算电子从基态被阿秒脉冲电离到连续态的振幅。其中式(5)中的跃迁矩阵元 $d[\boldsymbol{p}+\boldsymbol{A}(t+\tau)]$ 是动量和时间的函数，不再视为常数处理，可以由 Hartree-Fock-Slater(HFS)模型中的有效原子势计算得出[110]。同时在积分计算跃迁振幅时采用更符合 SFA 近似的正交完备 Volkov 态作为基矢，取代之前方法普遍使用的平面波基矢。第二步，保留计算所得能谱的相位信息，并将实验能谱数据的强度映射到计算能谱。第三步，根据计算能谱和实验能谱构建最小误差函数，并通过 Brent 方法[111]优化误差函数给出迭代结果。重复以上 3 个步骤直至达到收敛条件，实现阿秒脉冲和红外调制场的反演。

虽然 VTGPA 仍采用构造误差函数并迭代优化的求解方法，但其计算过程仅使用 SFA 近似而规避了 CMA 等诸多近似条件，大大拓展了算法的适用范围。该算法可以同时重建阿秒脉冲和复杂红外脉冲波形。仿真和实验数据反演结果表明，相较于 FROG-CRAB 方法，VTGPA 的反演谱图和输入谱图的均方误差可以降低 3 个量级。

当阿秒脉冲谱宽延伸到软 X 射线频段时，产生和测量阿秒脉冲都会存在更复杂的物理过程。Gaumnitz 等[27]研究了多个束缚态电子电离对阿秒能谱的非相干贡献，在 VTGPA 的基础上提出了多线 VTGPA(ML-VTGPA)算法，并在实验上使用双周期中红外驱动电场作用于氙气得到覆盖 65～150 eV 的宽带阿秒能谱。最终通过 ML-VTGPA 反演得到 $\tau_{\mathrm{SXR}}=43\pm1$ as 的软 X 射线波段超短阿秒脉冲，以及 $\tau_{\mathrm{mid-IR}}=11.1\pm0.7$ fs 的中红外脉冲，并通过与瞬态光栅 FROG(TG-FROG)[112]方法测量的红外脉冲波形和脉宽对比，验证了反演的准确性。该工作如图 8 所示。

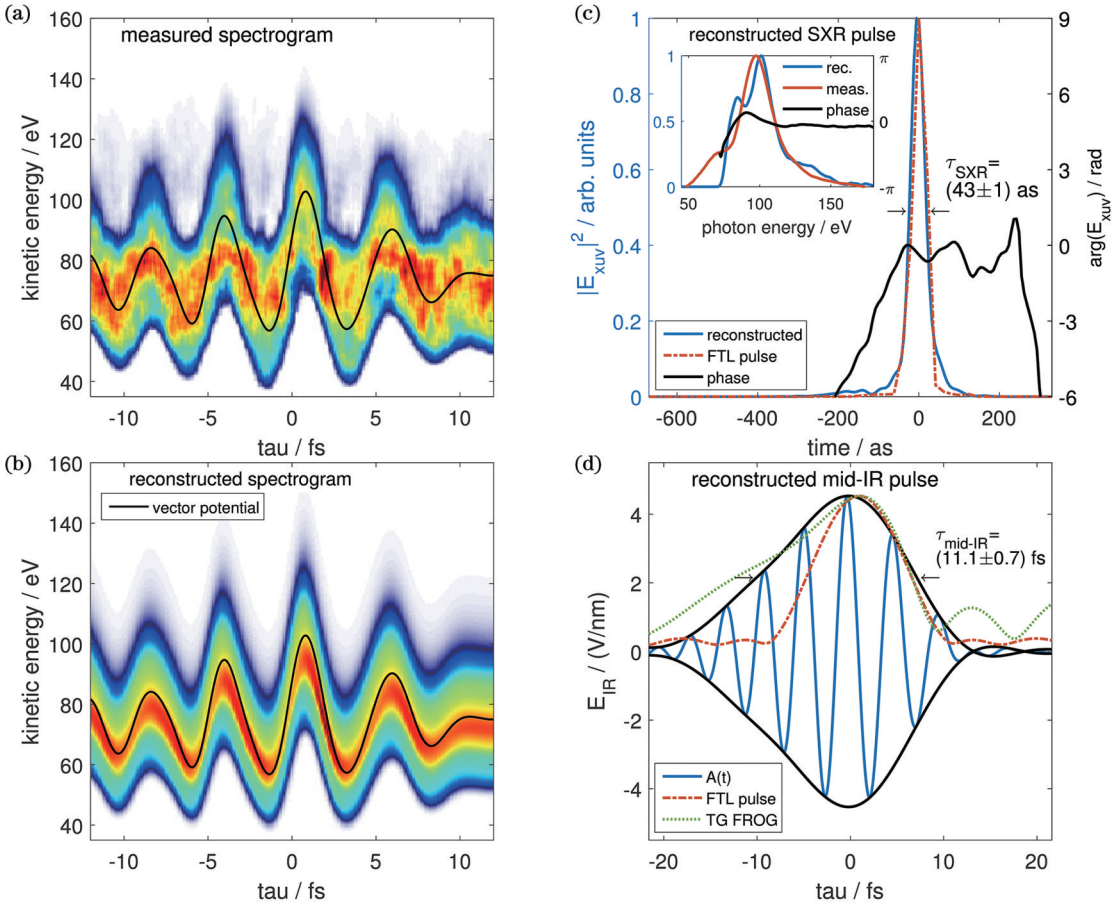

图 8　ML-VTGPA 反演实验阿秒条纹谱及表征 43 as 单个阿秒脉冲。(a)实验测量阿秒条纹谱；(b)ML-VTGPA 重建条纹谱及中红外脉冲矢势；(c)重建(蓝色)和傅里叶变换极限(FTL)(红色)表征所得 IAP 时域振幅及相位(黑色)，插图为测量(红色)和重建(蓝色)SXR 脉冲的光谱及相位(黑色)；(d)重建(蓝色)和 FTL(红色)及 TG-FROG 测量(绿色)的中红外脉冲矢势[27]

Fig. 8　Reconstruction of 43 as IAP spectrogram. (a) Experimentally measured attosecond streaking spectrogram with target gas xenon; (b) reconstructed spectrogram and mid-IR vector potential by ML-VTGPA; (c) reconstructed (blue) and Fourier transform limited (FTL) (red dashed) IAP temporal amplitude with temporal phase (black), where inset shows retrieved spectrum (blue) compared with measured spectrum (red) and retrieved spectral phase (black); (d) reconstructed mid-IR vector potential (blue), FTL pulse amplitude (red dashed) and TG-FROG measured amplitude (green dotted)[27]

3.5 PROBP

基于SFA近似理论，Lin小组提出针对宽带阿秒反演的PROBP，以及改进的自相关PROBP（PROBP-AC），使用条纹能谱的时间自相关函数检验重建阿秒脉冲的正确性[98-99]。为了更符合宽带能谱作用下电子光电离截面的实际情况，采用单电子近似计算跃迁矩阵元，并直接对式(5)进行积分计算，避免了引入诸多近似带来的误差。

PROBP方法仍然采用迭代算法反演阿秒脉冲相位和红外电场波形，通过B样条拟合给出猜测阿秒脉冲相位、红外电场包络和相位作为初值，然后代入光电子振幅公式(5)直接积分计算得到条纹能谱$S_1(E,\tau)$，通过与实验条纹能谱$S_0(E,\tau)$对比，构造误差函数$E[a_i,b_i,c_i]=\sum_{k,l}\left[S_0(E_k,\tau_l)-S_1(E_k,\tau_l)\right]^2$，最后采用基因算法寻优求解插值系数，使得误差函数达到最小值或达到收敛条件，通过最优插值系数就可以从B样条插值函数中重建阿秒脉冲和红外电场矢势。

为了检验反演结果的准确性，通常是将反演所得的阿秒脉冲和红外调制脉冲结合，根据强场近似下的式(5)计算阿秒条纹谱，通过比较实验与反演条纹谱的差别，能够一定程度上验证反演的准确性。PROBP-AC算法通过数值实验表明，对于给定的具有超宽带频谱的阿秒脉冲，不同的频谱啁啾会极大地影响其脉冲宽度，然而仿真计算所得阿秒条纹谱差别不明显。该算法中提出通过计算对比实验和反演的阿秒条纹谱自相关系数，验证反演准确性：

$$Q(\tau_1,\tau_2)=\int_0^{\infty}S(E,\tau_1)S(E,\tau_2)\mathrm{d}E。\tag{13}$$

PROBP和PROBP-AC方法通过数值实验，表明其对于软X射线到水窗波段290～530 eV的超宽带阿秒脉冲和宽频谱红外电场的表征能力，并尝试绕过SFA近似公式(5)，通过直接求解含时薛定谔方程（TDSE）获得条纹能谱，能够克服SFA在低能电子谱段的误差。但其采用B样条插样方法导致只能应用于光滑变化的光谱相位，无法应对实验中常见的振动等机械因素导致的阿秒光谱相位跳变，且该算法依赖于实验上无红外电场测量的阿秒脉冲光谱强度和红外电场信息，对实验测量的噪声较为敏感。

随着近些年中红外激光器和少周期脉冲技术的发展，在2017年有3个研究组分别报道产生并测量了软X射线谱段的单个阿秒脉冲[27-28,113]。通过使用PROBP-AC算法，Zhao等[99]对3组阿秒谱图数据进行表征和分析，并计算其条纹能谱的自相关函数。如图9所示，其引用的文献中重建条纹能谱[图9(b)]与实验条纹能谱[图9(a)]的自相关函数相差较大，且其引用的文献中重建的43 as单个阿秒脉冲波形与光谱相位[图9(d)和图9(e)]，与PROBP-AC重建结果显示的62 as和相位也有较大不同。

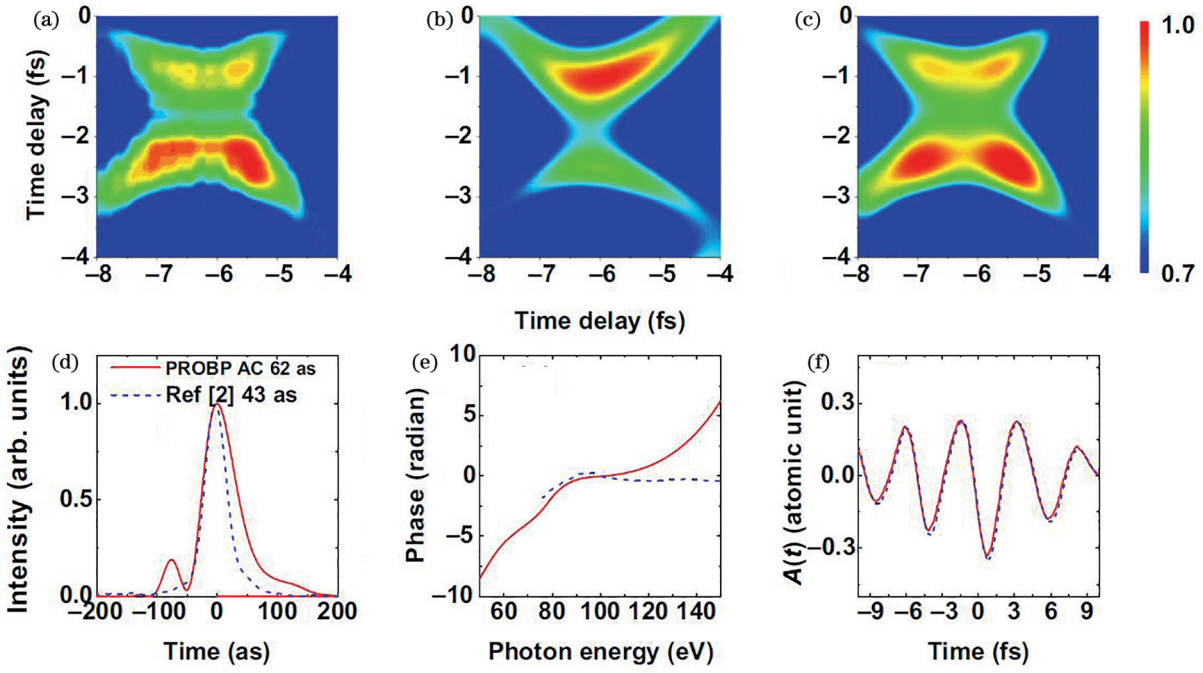

图9 PROBP-AC方法。(a)，(b)文献中实验测量及重建的阿秒条纹谱计算所得自相关函数；(c)PROBP-AC算法重建阿秒条纹谱的自相关函数；(d)～(f)PROBP-AC算法与文献中ML-VTGPA重建的阿秒脉冲波形、光谱相位以及红外电场矢势[99]

Fig. 9 PROBP-AC method. (a), (b) Autocorrelation (AC) patterns extracted from experimental and reconstructed spectrogram from literature; (c) AC pattern retrieved by PROBP-AC; (d)–(f) reconstructed results from ML-VTGPA in literature compared with PROBP-AC for IAP envelope, spectral phase and IR vector potential[99]

可以看出，对于极紫外乃至软X射线波段的超宽带阿秒脉冲，提高测量与反演的准确性仍然是富有挑战性的课题，且由于实验方案及反演算法差异性较大，目前还缺少适用于多种阿秒脉冲光谱、相位和波形的普适性算法。同时需要发展能够更加有效地判断反演准确性的方法。

3.6 神经网络与机器学习

近年迅速发展的神经网络为阿秒脉冲表征提供了新的思路。常增虎小组使用仿真阿秒条纹能谱及输入阿秒脉冲波形训练神经网络模型，建立能谱和阿秒脉冲波形间的映射函数，然后再用于映射实验能谱以反演阿秒脉冲频谱相位及时域波形[100-102,114]。

神经网络模型中包含大小由输入参数决定的卷积层，每个卷积层由权重矩阵组成，将根据SFA公式(5)计算得到的大量谱图数据作为数据集输入神经网络模型，以输入值与神经网络反演的阿秒脉冲相位、红外电场信息构建误差函数，并采用最速下降方法的改进版Adam算法[115]，寻优求解误差函数。模型通过有监督学习训练权重矩阵系数，最终当误差函数收敛到全局最优解时神经网络模型训练完成，获得阿秒脉冲相位和红外电场矢势的反演结果，并与输入值进行对比，验证模型反演效果。当将已训练的神经网络模型应用于实验数据时，为了提高反演准确性，通过无监督学习调整模型权重参数，以实验能谱和模型反演能谱重新定义误差函数并采用Adam方法进行优化，误差函数收敛到极小时，表明对实验数据的成功反演。

神经网络方法优点在于通过大量仿真数据完成对模型的训练后，能够以远优于其他方法的速度反演实验谱图，但是其模型的映射过程缺乏清晰的物理图像，而且对于含有复杂噪声的实验数据，重建结果的准确性有待验证。

4 总结与展望

本文主要对基于阿秒条纹相机的单个阿秒脉冲表征技术进行了综述。FROG-CRAB算法是最早的单个阿秒脉冲表征算法，它将飞秒表征方法通过对跃迁偶极矩的简化及中心动量近似应用于阿秒表征，但其应用限制在窄带阿秒脉冲的范围。层析投影算法巧妙地将层析算法中的相位反演技术引入阿秒领域，放宽了对能谱数据采样的限制，但仍局限于中心动量近似。PROOF提出了单频滤波思想，更加适用于宽带阿秒脉冲表征，但其采用的遗传算法效率低下。我们提出的qPROOF算法在适用范围、反演精度和速度上都较PROOF有较大提升。VTGPA在迭代过程中绕过傅里叶变换从而避免了中心动量近似，且更准确地引入跃迁矩阵元，没有额外对脉冲形式施加限制，能够同时表征复杂飞秒调制场和阿秒脉冲。PROBP-AC使用能谱自相关函数简化目标函数，提高了反演速度和准确性，提出求解TDSE以获得能谱数据，绕过SFA近似能够提高在低能电子情形下的准确性，但反演算法仍基于SFA近似，因此引入TDSE的合理性仍需更多理论和实验证明。神经网络算法提供了新的反演思路，能够直接建立能谱与阿秒相位的映射，但缺乏直观的物理图像。

综上所述，阿秒脉冲的表征算法在近20年内有了长足发展。理论上，对跃迁矩阵元从常值处理到HFS理论计算给出，对能谱正向计算提出使用强场近似、中心动量近似、慢变包络近似、弱场近似等进行简化处理，再到求解TDSE，越来越符合真实物理含义。相位反演算法上，从中心投影算法改进到基因算法，再到神经网络映射，反演速度更快、结果更准确、鲁棒性更好，但这些算法都有各自的局限性，反演结果的准确性缺乏统一的方法进行验证。

另外，阿秒条纹相机技术有其固有缺陷。其能量分辨率以及气体介质的光电离截面随光子能量提高而降低，对于软X射线波段的超宽带阿秒脉冲测量过程中误差较大，导致其时间分辨率具有上限，要实现更高的时间分辨率就需要提高调制场强度，进而将不可避免地导致靶气体直接电离，引入更多的噪声。而且实验上机械振动等不可避免因素会导致阿秒脉冲和红外脉冲间的时间抖动、阿秒脉冲相位跳变等，目前已有的算法对于这些因素的适用性还需检验和提升。

因此可见，阿秒表征算法仍有很大的发展前景。目前的反演算法主要集中于阿秒谱宽在数十至数百电子伏特范围内。随着人们对原子分子内壳层电子动力学和更复杂材料、生物结构研究的需求的增加，以及高重复频率、高能量、中红外波长驱动光的发展和应用，产生的超宽带阿秒脉冲已经从数十电子伏特拓展至水窗波段，覆盖了碳、氮、氧、氯等众多元素K吸收边。为了更准确地表征极紫外阿秒脉冲脉宽及时域特征，继而更深入地应用阿秒脉冲，对于超宽带阿秒脉冲的表征算法仍需投入更多研究精力。

参 考 文 献

[1] Zewail A H. Laser femtochemistry[M]. Singapore: World Scientific, 1994: 25-33.

[2] Ferray M, L'Huillier A, Li X F, et al. Multiple-harmonic conversion of 1064 nm radiation in rare gases[J]. Journal of Physics B: Atomic, Molecular and Optical Physics, 1988, 21(3): L31-L35.

[3] McPherson A, Gibson G, Jara H, et al. Studies of multiphoton production of vacuum-ultraviolet radiation in the rare gases[J]. Journal of the Optical Society of America B, 1987, 4(4): 595-601.

[4] Corkum P B. Plasma perspective on strong field multiphoton ionization[J]. Physical Review Letters, 1993, 71(13): 1994-1997.

[5] Arpin P, Popmintchev T, Wagner N L, et al. Enhanced high harmonic generation from multiply ionized argon above 500 eV through laser pulse self-compression[J]. Physical Review Letters, 2009, 103(14): 143901.

[6] Luu T T, Yin Z, Jain A, et al. Extreme-ultraviolet high-harmonic generation in liquids[J]. Nature Communications, 2018, 9: 3723.

[7] 戴晨, 汪洋, 缪志明, 等. 基于飞秒激光与物质相互作用的高次谐波产生及应用[J]. 激光与光电子学进展, 2021, 58(3): 0300001.
Dai C, Wang Y, Miao Z M, et al. Generation and application of

high-order harmonics based on interaction between femtosecond laser and matter[J]. Laser & Optoelectronics Progress, 2021, 58(3): 0300001.

[8] Gao J X, Wu J Q, Lou Z Y, et al. High-order harmonic generation in an X-ray range from laser-induced multivalent ions of noble gas [J]. Optica, 2022, 9(9): 1003-1008.

[9] 赵旭琳, 白丽华, 白亚, 等. 双色激光场作用下水的高次谐波光谱移动[J]. 光学学报, 2023, 43(13): 1326002.
Zhao X L, Bai L H, Bai Y, et al. High-harmonic spectral shift of water under two-color laser fields[J]. Acta Optica Sinica, 2023, 43(13): 1326002.

[10] 于术娟, 刘竹琴, 刘艳峰, 等. 通过奇偶谐波谱重构不对称平面分子的构型[J]. 激光与光电子学进展, 2023, 60(1): 0102002.
Yu S J, Liu Z Q, Liu Y F, et al. Probing the structure of asymmetric planar molecules using odd-even high harmonics[J]. Laser & Optoelectronics Progress, 2023, 60(1): 0102002.

[11] Mondal A, Neufeld O, Yin Z, et al. High-harmonic spectroscopy of low-energy electron-scattering dynamics in liquids[J]. Nature Physics, 2023, 19: 1813-1820.

[12] Mondal A, Waser B, Balciunas T, et al. High-harmonic generation in liquids with few-cycle pulses: effect of laser-pulse duration on the cut-off energy[J]. Optics Express, 2023, 31(21): 34348-34361.

[13] Li S, Tang Y G, Ortmann L, et al. High-order harmonic generation from a thin film crystal perturbed by a quasi-static terahertz field[J]. Nature Communications, 2023, 14: 2603.

[14] Tcherbakoff O, Mével E, Descamps D, et al. Time-gated high-order harmonic generation[J]. Physical Review A, 2003, 68(4): 043804.

[15] Sola I J, Mével E, Elouga L, et al. Controlling attosecond electron dynamics by phase-stabilized polarization gating[J]. Nature Physics, 2006, 2: 319-322.

[16] Mashiko H, Gilbertson S, Li C Q, et al. Double optical gating of high-order harmonic generation with carrier-envelope phase stabilized lasers[J]. Physical Review Letters, 2008, 100(10): 103906.

[17] Gilbertson S, Mashiko H, Li C Q, et al. A low-loss, robust setup for double optical gating of high harmonic generation[J]. Applied Physics Letters, 2008, 92(7): 071109.

[18] Calegari F, Lucchini M, Negro M, et al. Temporal gating methods for the generation of isolated attosecond pulses[J]. Journal of Physics B: Atomic, Molecular and Optical Physics, 2012, 45(7): 074002.

[19] Timmers H, Sabbar M, Kobayashi Y, et al. Polarization assisted amplitude gating as a route to tunable, high-contrast single attosecond pulses[J]. Optica, 2016, 3(7): 707-710.

[20] Paul P M, Toma E S, Breger P, et al. Observation of a train of attosecond pulses from high harmonic generation[J]. Science, 2001, 292(5522): 1689-1692.

[21] Hentschel M, Kienberger R, Spielmann C, et al. Attosecond metrology[J]. Nature, 2001, 414(6863): 509-513.

[22] Wang J C, Xiao F, Wang L, et al. Fast phase retrieval for broadband attosecond pulse characterization[J]. Optics Express, 2023, 31(26): 43224-43233.

[23] Zhong S Y, Teng H, Zhu X X, et al. Characterizing 86-attosecond isolated pulses based on amplitude gating of high harmonic generation[J]. Chinese Optics Letters, 2023, 21(11): 113201.

[24] Kienberger R, Goulielmakis E, Uiberacker M, et al. Atomic transient recorder[J]. Nature, 2004, 427(5429): 817-821.

[25] 王向林, 徐鹏, 李捷, 等. 利用自研阿秒条纹相机测得159as孤立阿秒脉冲[J]. 中国激光, 2020, 47(4): 0415002.
Wang X L, Xu P, Li J, et al. Isolated attosecond pulse with 159 as duration measured by home built attosecond streaking camera[J]. Chinese Journal of Lasers, 2020, 47(4): 0415002.

[26] Wang X W, Wang L, Xiao F, et al. Generation of 88 as isolated attosecond pulses with double optical gating[J]. Chinese Physics Letters, 2020, 37(2): 023201.

[27] Gaumnitz T, Jain A, Pertot Y, et al. Streaking of 43-attosecond soft-X-ray pulses generated by a passively CEP-stable mid-infrared driver[J]. Optics Express, 2017, 25(22): 27506-27518.

[28] Li J, Ren X M, Yin Y C, et al. 53-attosecond X-ray pulses reach the carbon K-edge[J]. Nature Communications, 2017, 8: 186.

[29] Zhan M J, Ye P, Teng H, et al. Generation and measurement of isolated 160-attosecond XUV laser pulses at 82 eV[J]. Chinese Physics Letters, 2013, 30(9): 093201.

[30] Zhao K, Zhang Q, Chini M, et al. Tailoring a 67 attosecond pulse through advantageous phase-mismatch[J]. Optics Letters, 2012, 37(18): 3891-3893.

[31] Goulielmakis E, Schultze M, Hofstetter M, et al. Single-cycle nonlinear optics[J]. Science, 2008, 320(5883): 1614-1617.

[32] Sansone G, Benedetti E, Calegari F, et al. Isolated single-cycle attosecond pulses[J]. Science, 2006, 314(5798): 443-446.

[33] Mashiko H, Gilbertson S, Chini M, et al. Extreme ultraviolet supercontinua supporting pulse durations of less than one atomic unit of time[J]. Optics Letters, 2009, 34(21): 3337-3339.

[34] Popmintchev T, Chen M C, Popmintchev D, et al. Bright coherent ultrahigh harmonics in the keV X-ray regime from mid-infrared femtosecond lasers[J]. Science, 2012, 336(6086): 1287-1291.

[35] Mashiko H, Oguri K, Sogawa T. Attosecond pulse generation in carbon K-edge region (284 eV) with sub-250 μJ driving laser using generalized double optical gating method[J]. Applied Physics Letters, 2013, 102(17): 171111.

[36] Teichmann S M, Silva F, Cousin S L, et al. 0.5-keV soft X-ray attosecond continua[J]. Nature Communications, 2016, 7: 11493.

[37] Drescher M, Hentschel M, Kienberger R, et al. Time-resolved atomic inner-shell spectroscopy[J]. Nature, 2002, 419(6909): 803-807.

[38] Liu J P, Li Y Q, Wang L, et al. Coherent control of atomic inner-shell X-ray lasing via perturbed valence-shell transitions[J]. Physical Review A, 2021, 104(3): L031101.

[39] Schultze M, Fiess M, Karpowicz N, et al. Delay in photoemission [J]. Science, 2010, 328(5986): 1658-1662.

[40] Vos J, Cattaneo L, Patchkovskii S, et al. Orientation-dependent stereo Wigner time delay and electron localization in a small molecule[J]. Science, 2018, 360(6395): 1326-1330.

[41] Nandi S, Plésiat E, Zhong S, et al. Attosecond timing of electron emission from a molecular shape resonance[J]. Science Advances, 2020, 6(31): eaba7762.

[42] Biswas S, Förg B, Ortmann L, et al. Probing molecular environment through photoemission delays[J]. Nature Physics, 2020, 16: 778-783.

[43] Calegari F, Ayuso D, Trabattoni A, et al. Ultrafast electron dynamics in phenylalanine initiated by attosecond pulses[J]. Science, 2014, 346(6207): 336-339.

[44] Kraus P M, Mignolet B, Baykusheva D, et al. Measurement and laser control of attosecond charge migration in ionized iodoacetylene [J]. Science, 2015, 350(6262): 790-795.

[45] Yong H W, Sun S C, Gu B, et al. Attosecond charge migration in molecules imaged by combined X-ray and electron diffraction[J]. Journal of the American Chemical Society, 2022, 144(45): 20710-20716.

[46] He L X, Sun S Q, Lan P F, et al. Filming movies of attosecond charge migration in single molecules with high harmonic spectroscopy[J]. Nature Communications, 2022, 13: 4595.

[47] He L X, He Y Q, Sun S Q, et al. Attosecond probing and control of charge migration in carbon-chain molecule[J]. Advanced Photonics, 2023, 5: 056001.

[48] Johnson A S, Perez-Salinas D, Siddiqui K M, et al. Ultrafast X-ray imaging of the light-induced phase transition in VO_2[J]. Nature Physics, 2023, 19: 215-220.

[49] Mashiko H, Oguri K, Yamaguchi T, et al. Petahertz optical drive with wide-bandgap semiconductor[J]. Nature Physics, 2016, 12: 741-745.

[50] Garg M, Zhan M, Luu T T, et al. Multi-petahertz electronic metrology[J]. Nature, 2016, 538(7625): 359-363.
[51] Mashiko H, Chisuga Y, Katayama I, et al. Multi-petahertz electron interference in Cr: Al_2O_3 solid-state material[J]. Nature Communications, 2018, 9: 1468.
[52] Gong X C, Heck S, Jelovina D, et al. Attosecond spectroscopy of size-resolved water clusters[J]. Nature, 2022, 609(7927): 507-511.
[53] Yin Z, Chang Y P, Balčiūnas T, et al. Femtosecond proton transfer in urea solutions probed by X-ray spectroscopy[J]. Nature, 2023, 619(7971): 749-754.
[54] Kim K T, Zhang C M, Shiner A D, et al. Manipulation of quantum paths for space-time characterization of attosecond pulses [J]. Nature Physics, 2013, 9: 159-163.
[55] Kim K T, Zhang C M, Ruchon T, et al. Photonic streaking of attosecond pulse trains[J]. Nature Photonics, 2013, 7: 651-656.
[56] Wheeler J A, Borot A, Monchocé S, et al. Attosecond lighthouses from plasma mirrors[J]. Nature Photonics, 2012, 6: 829-833.
[57] Vincenti H, Quéré F. Attosecond lighthouses: how to use spatiotemporally coupled light fields to generate isolated attosecond pulses[J]. Physical Review Letters, 2012, 108(11): 113904.
[58] He L X, Hu J C, Sun S Q, et al. All-optical spatio-temporal metrology for isolated attosecond pulses[J]. Journal of Physics B: Atomic, Molecular and Optical Physics, 2022, 55(20): 205601.
[59] Yang Z, Cao W, Mo Y L, et al. All-optical attosecond time domain interferometry[J]. National Science Review, 2020, 8(10): nwaa211.
[60] Yang Z, Cao W, Chen X, et al. All-optical frequency-resolved optical gating for isolated attosecond pulse reconstruction[J]. Optics Letters, 2020, 45(2): 567-570.
[61] Mairesse Y, Gobert O, Breger P, et al. High harmonic XUV spectral phase interferometry for direct electric-field reconstruction [J]. Physical Review Letters, 2005, 94(17): 173903.
[62] Cormier E, Walmsley I A, Kosik E M, et al. Self-referencing, spectrally, or spatially encoded spectral interferometry for the complete characterization of attosecond electromagnetic pulses[J]. Physical Review Letters, 2005, 94(3): 033905.
[63] Itatani J, Quéré F, Yudin G L, et al. Attosecond streak camera[J]. Physical Review Letters, 2002, 88(17): 173903.
[64] 曹伟, 陆培祥. 基于高次谐波阿秒光源的超快测量技术(特邀)[J]. 光子学报, 2021, 50(8): 0850203.
Cao W, Lu P X. Ultrafast measurement techniques using high-order harmonic based attosecond light sources (invited)[J]. Acta Photonica Sinica, 2021, 50(8): 0850203.
[65] 魏志义, 钟诗阳, 贺新奎, 等. 阿秒光学进展及发展趋势[J]. 中国激光, 2021, 48(5): 0501001.
Wei Z Y, Zhong S Y, He X K, et al. Progresses and trends in attosecond optics[J]. Chinese Journal of Lasers, 2021, 48(5): 0501001.
[66] Krausz F, Ivanov M. Attosecond physics[J]. Reviews of Modern Physics, 2009, 81(1): 163-234.
[67] 赵昆, 高亦谈, 朱孝先, 等. 阿秒脉冲测量原理和技术研究进展[J]. 科学通报, 2021, 66(8): 835-846.
Zhao K, Gao Y T, Zhu X X, et al. Principle and technology of attosecond pulse characterization[J]. Chinese Science Bulletin, 2021, 66(8): 835-846.
[68] Li J, Lu J, Chew A, et al. Attosecond science based on high harmonic generation from gases and solids[J]. Nature Communications, 2020, 11: 2748.
[69] Orfanos I, Makos I, Liontos I, et al. Attosecond pulse metrology [J]. APL Photonics, 2019, 4(8): 080901.
[70] Young L, Ueda K, Gühr M, et al. Roadmap of ultrafast X-ray atomic and molecular physics[J]. Journal of Physics B: Atomic, Molecular and Optical Physics, 2018, 51(3): 032003.
[71] Calegari F, Sansone G, Stagira S, et al. Advances in attosecond science[J]. Journal of Physics B: Atomic, Molecular and Optical Physics, 2016, 49(6): 062001.
[72] Chang Z H, Corkum P B, Leone S R. Attosecond optics and technology: progress to date and future prospects[J]. Journal of the Optical Society of America B, 2016, 33(6): 1081-1097.
[73] Gallmann L, Cirelli C, Keller U. Attosecond science: recent highlights and future trends[J]. Annual Review of Physical Chemistry, 2012, 63: 447-469.
[74] Sansone G, Poletto L, Nisoli M. High-energy attosecond light sources[J]. Nature Photonics, 2011, 5: 655-663.
[75] Zhao Z X, Chang Z H, Tong X M, et al. Circularly-polarized laser-assisted photoionization spectra of argon for attosecond pulse measurements[J]. Optics Express, 2005, 13(6): 1966-1977.
[76] Li S Q, Guo Z H, Coffee R N, et al. Characterizing isolated attosecond pulses with angular streaking[J]. Optics Express, 2018, 26(4): 4531-4547.
[77] Hartmann N, Hartmann G, Heider R, et al. Attosecond time-energy structure of X-ray free-electron laser pulses[J]. Nature Photonics, 2018, 12: 215-220.
[78] Zhao X, Li S Q, Driver T, et al. Characterization of single-shot attosecond pulses with angular streaking photoelectron spectra[J]. Physical Review A, 2022, 105(1): 013111.
[79] Goulielmakis E, Loh Z H, Wirth A, et al. Real-time observation of valence electron motion[J]. Nature, 2010, 466(7307): 739-743.
[80] Cavalieri A L, Müller N, Uphues T, et al. Attosecond spectroscopy in condensed matter[J]. Nature, 2007, 449(7165): 1029-1032.
[81] Kovács K, Tosa V. Macroscopic attosecond chirp compensation [J]. Optics Express, 2019, 27(15): 21872-21879.
[82] Chang Z H. Attosecond chirp compensation in water window by plasma dispersion[J]. Optics Express, 2018, 26(25): 33238-33244.
[83] Ko D H, Kim K T, Nam C H. Attosecond-chirp compensation with material dispersion to produce near transform-limited attosecond pulses[J]. Journal of Physics B: Atomic, Molecular and Optical Physics, 2012, 45(7): 074015.
[84] Kim K T, Kang K S, Park M N, et al. Self-compression of attosecond high-order harmonic pulses[J]. Physical Review Letters, 2007, 99(22): 223904.
[85] Morlens A S, Balcou P, Zeitoun P, et al. Compression of attosecond harmonic pulses by extreme-ultraviolet chirped mirrors [J]. Optics Letters, 2005, 30(12): 1554-1556.
[86] Kim K T, Kim C M, Baik M G, et al. Single sub-50-attosecond pulse generation from chirp-compensated harmonic radiation using material dispersion[J]. Physical Review A, 2004, 69(5): 051805.
[87] Yakovlev V S, Gagnon J, Karpowicz N, et al. Attosecond streaking enables the measurement of quantum phase[J]. Physical Review Letters, 2010, 105(7): 073001.
[88] Han M, Ji J B, Balčiūnas T, et al. Attosecond circular-dichroism chronoscopy of electron vortices[J]. Nature Physics, 2023, 19: 230-236.
[89] Reduzzi M, Carpeggiani P, Kühn S, et al. Advances in high-order harmonic generation sources for time-resolved investigations[J]. Journal of Electron Spectroscopy and Related Phenomena, 2015, 204: 257-268.
[90] Uiberacker M, Uphues T, Schultze M, et al. Attosecond real-time observation of electron tunnelling in atoms[J]. Nature, 2007, 446(7136): 627-632.
[91] Gagnon J, Goulielmakis E, Yakovlev V S. The accurate FROG characterization of attosecond pulses from streaking measurements [J]. Applied Physics B, 2008, 92(1): 25-32.
[92] Mairesse Y, Quéré F. Frequency-resolved optical gating for complete reconstruction of attosecond bursts[J]. Physical Review A, 2005, 71(1): 011401.
[93] Chini M, Gilbertson S, Khan S D, et al. Characterizing ultrabroadband attosecond lasers[J]. Optics Express, 2010, 18(12): 13006-13016.
[94] Lucchini M, Lucarelli G D, Murari M, et al. Few-femtosecond extreme-ultraviolet pulses fully reconstructed by a ptychographic technique[J]. Optics Express, 2018, 26(6): 6771-6784.

[95] Lucchini M, Nisoli M. Refined ptychographic reconstruction of attosecond pulses[J]. Applied Sciences, 2018, 8(12): 2563.
[96] Lucchini M, Brügmann M H, Ludwig A, et al. Ptychographic reconstruction of attosecond pulses[J]. Optics Express, 2015, 23(23): 29502-29513.
[97] Keathley P D, Bhardwaj S, Moses J, et al. Volkov transform generalized projection algorithm for attosecond pulse characterization[J]. New Journal of Physics, 2016, 18(7): 073009.
[98] Zhao X, Wei H, Wu Y, et al. Phase-retrieval algorithm for the characterization of broadband single attosecond pulses[J]. Physical Review A, 2017, 95(4): 043407.
[99] Zhao X, Wang S J, Yu W W, et al. Metrology of time-domain soft X-ray attosecond pulses and reevaluation of pulse durations of three recent experiments[J]. Physical Review Applied, 2020, 13(3): 034043.
[100] Brunner C, Duensing A, Schröder C, et al. Deep learning in attosecond metrology[J]. Optics Express, 2022, 30(9): 15669-15684.
[101] Nishizaki Y, Horisaki R, Kitaguchi K, et al. Analysis of non-iterative phase retrieval based on machine learning[J]. Optical Review, 2020, 27(1): 136-141.
[102] White J, Chang Z H. Attosecond streaking phase retrieval with neural network[J]. Optics Express, 2019, 27(4): 4799-4807.
[103] Kane D J, Trebino R. Characterization of arbitrary femtosecond pulses using frequency-resolved optical gating[J]. IEEE Journal of Quantum Electronics, 1993, 29(2): 571-579.
[104] Sweetser J N, Fittinghoff D N, Trebino R. Transient-grating frequency-resolved optical gating[J]. Optics Letters, 1997, 22(8): 519-521.
[105] Kane D J. Real-time measurement of ultrashort laser pulses using principal component generalized projections[J]. IEEE Journal of Selected Topics in Quantum Electronics, 1998, 4(2): 278-284.
[106] Xue B, Midorikawa K, Takahashi E J. Gigawatt-class, tabletop, isolated-attosecond-pulse light source[J]. Optica, 2022, 9(4): 360-363.
[107] Hoppe W. Beugung im inhomogenen primärstrahlwellenfeld. I. prinzip einer phasenmessung von elektronenbeungungsinterferenzen [J]. Acta Crystallographica Section A, 1969, 25(4): 495-501.
[108] Rodenburg J M, Hurst A C, Cullis A G. Transmission microscopy without lenses for objects of unlimited size[J]. Ultramicroscopy, 2007, 107(2/3): 227-231.
[109] Laurent G, Cao W, Ben-Itzhak I, et al. Attosecond pulse characterization[J]. Optics Express, 2013, 21(14): 16914-16927.
[110] Bhardwaj S, Son S K, Hong K H, et al. Recombination-amplitude calculations of noble gases, in both length and acceleration forms, beyond the strong-field approximation[J]. Physical Review A, 2013, 88(5): 053405.
[111] Anderson D. Algorithms for minimization without derivatives[J]. IEEE Transactions on Automatic Control, 1974, 19(5): 632-633.
[112] Pirozhkov A S, Mori M, Ogura K, et al. Transient-grating FROG for measurement of sub-10-fs to few-ps amplified pulses[C]// Advanced Solid-State Photonics 2008, January 27-30, 2008, Nara. Washington, DC: OSA, 2008: MC8.
[113] Cousin S L, Di Palo N, Buades B, et al. Attosecond streaking in the water window: a new regime of attosecond pulse characterization[J]. Physical Review X, 2017, 7(4): 041030.
[114] Zahavy T, Dikopoltsev A, Cohen O, et al. Deep learning reconstruction of ultrashort pulses[C]//2018 Conference on Lasers and Electro-Optics (CLEO), May 13-18, 2018, San Jose, CA, USA. New York: IEEE Press, 2018.
[115] Kingma D P, Ba J. Adam: a method for stochastic optimization [EB/OL]. (2014-12-22) [2023-11-09]. http://arxiv.org/abs/1412.6980.

Research Progress of Isolated Attosecond Pulse Characterization

Wang Jiacan[1,2], Xiao Fan[1,2], Wang Xiaowei[1,2**], Wang Li[1,2], Tao Wenkai[1,2], Zhao Lingyi[1,2], Li Xi'ao[1,2], Zhao Zengxiu[1,2*]

[1]*College of Science, National University of Defense Technology, Changsha* 410073, *Hunan, China*;
[2]*Hunan Key Laboratory of Extreme Matter and Applications, National University of Defense Technology, Changsha* 410073, *Hunan, China*

Abstract

Significance In 2023, Pierre Agostini, Ference Krausz and Anne L'Huillier had been awarded the Nobel Prize in Physics for their contribution in experimental methods of generating attosecond pulses of light for the study of electron dynamics in matter. Based on their pioneering work of high harmonics generation (HHG), generation and characterization of attosecond pulse trains (APTs) and isolated attosecond pulses (IAPs), a whole new physics research field named attosecond science was opened up. With the rapid development of attosecond science in the past two decades, extremely short IAPs have been generated and applied in photon spectroscopy and attosecond transient absorption spectroscopy (ATAS), providing researchers more powerful tool to study the ultrafast electron dynamics in atoms, molecules and condensed matter than ever with attosecond temporal resolution. These ultrafast processes include the photoionization time delay in atoms, ionization difference of polar and non-polar molecules, electrons migration in multi-atomic molecules, measurement of Auger decay process, inner-shell transition and probing of multielectron dynamics.

Progress Thanks to the progress of the ultrafast laser techniques as pumping lasers, multiple methods for gating, and fine spectral chirp for compensation in the past two decades, the spectrum of the IAP has expanded from tens of electron volts to hundreds of electron volts and its pulse duration record is getting compressed. Although many research groups have succeeded in achievement of

broadband spectrum and appropriate dispersion compensation, generating sub-100 as (1 as = 10^{-18} s) IAP with world record 43 as, precise characterization is the basis of further study and applications of IAP. Firstly in 2001, the reconstruction of attosecond beating by interference of two-photon transitions (RABBITT) and model analysis method were proposed independently for characterization of half-cycle separated 250 as duration APTs and IAP with 650 as pulse duration respectively.

For the accurate measurement of such short attosecond pulses, the attosecond streaking camera scheme is adopted from the femtosecond pulses measurement in 2002. Based on the cross-correlation scheme, the IAP photoionized electrons are modulated in the presence of the delay controllable near-infrared (NIR) light field. And both the spectral phase and intensity distribution of IAP and NIR are encoded in the detected frequency and delay time two-dimensional measurement, denoted as spectrogram, which permits full reconstruction of the IAP and NIR.

Based on the attosecond streaking camera, many techniques have been proposed to retrieve the spectral phase and then reconstruct the temporal electric field of IAP and NIR. Developed by Mairesse *et al.*, the frequency-resolved optical gating for complete reconstruction of attosecond bursts (FROG-CRAB) is commonly used for attosecond pulse characterization. But it uses high intensity streaking fields, resulting in the above-threshold ionized electrons that could overlap with streaked electrons. Much worse is the central momentum approximation (CMA) used to apply the iterative algorithms in femtosecond laser measurement, which limits the IAP bandwidth to few electron volts. For circumventing the CMA, Chini *et al*. proposed the phase retrieval by omega oscillation filtering (PROOF) for broader bandwidth and shorter IAP. PROOF applies weak field approximation (WFA) to modulate the photoelectrons and therefore focuses on the oscillation component of the dressing laser frequency, while WFA limits the streaking and retrieval application and its genetic algorithm has the problems of huge time cost and fatal shortcomings of multiple solutions in the iterative process. The quick version of PROOF (qPROOF) proposes a new error function to improve the retrieval accuracy and can be solved by the steepest descent method, improving the speed 5000 times faster than genetic algorithm. Moreover, qPROOF algorithm is numerically tested and proved to be robust against the pulse duration and intensity of streaking NIR, time-of-flight (TOF) electron detection noise, pump-probe delay jitter and large scanning step.

Multiple methods also have been proposed to avoid the CMA, WFA and slowly varying envelope approximation. The Volkov transform generalized projections algorithm (VTGPA) based on the Volkov states is developed to bypass the commonly used Fourier transform, making this method more applicable for complex IAP electric field waveform. Also, many groups have come up with novel approaches such as phase retrieval of broadband pulse (PROBP) and PROBP-autocorrelation (PROBP-AC), as well as ptychographic algorithm for attosecond reconstruction, and even the neural network and machine learning techniques are adopted to inject new solutions for attosecond measurement.

Conclusions and Prospects Since the advent of IAP generation, extensive efforts have been devoted to IAP experimental generation, measurement and characterization algorithm research mainly based on attosecond streaking camera scheme, paving the way for further attosecond application, such as ATAS and attosecond photoelectron spectroscopy.

With the development and application of high-repetition, high pulse energy mid-infrared laser, the attosecond streaking camera faces theoretical flaws as its energy resolution and photoionization cross-section of the gas medium decrease with the increase of photon energy. Also streaking camera based characterization algorithm should be verified and developed under these novel experimental conditions. Both theoretically and experimentally, there is urgent need for a new approach to accurately characterize the spectral and temporal properties of IAP with the latest driving laser and measurement techniques. And the single shot measurement and characterization of IAP is also of vital importance in high-energy laser drive facility with relatively lower repetition rate.

Key words nonlinear optics; isolated attosecond pulse; attosecond streaking camera; phase retrieval and characterization